Bull Volcanol (2007) 69:661–679
DOI 10.1007/s00445-006-0101-6

RESEARCH ARTICLE

The morphology and evolution of the Stromboli 2002–2003 lava flow field: an example of a basaltic flow field emplaced on a steep slope

L. Lodato · L. Spampinato · A. Harris · S. Calvari · J. Dehn · M. Patrick

Received: 30 August 2004 / Accepted: 20 July 2006 / Published online: 22 November 2006

Abstract The use of a hand-held thermal camera during the 2002–2003 Stromboli effusive eruption proved essential in tracking the development of flow field structures and in measuring related eruption parameters, such as the number of active vents and flow lengths. The steep underlying slope on which the flow field was emplaced resulted in a characteristic flow field morphology. This comprised a proximal shield, where flow stacking and inflation caused piling up of lava on the relatively flat ground of the vent zone, that fed a medial–distal lava flow field. This zone was characterized by the formation of lava tubes and tumuli forming a complex network of tumuli and flows linked by tubes. Most of the flow field was emplaced on extremely steep slopes and this had two effects. It caused flows to slide, as well as flow, and flow fronts to fail frequently, persistent flow front crumbling resulted in the production of an extensive debris field. Channel-fed flows were also characterized by development of excavated debris levees in this zone (Calvari et al. 2005). Collapse of lava flow fronts and inflation of the upper proximal lava shield made volume calculation very difficult. Comparison of the final field volume with that expecta by integrating the lava effusion rates through time suggests a loss of ~70% erupted lava by flow front crumbling and accumulation as debris flows below sea level. Derived relationships between effusion rate, flow length, and number of active vents showed systematic and correlated variations with time where spreading of volume between numerous flows caused an otherwise good correlation between effusion rate, flow length to break down. Observations collected during this eruption are useful in helping to understand lava flow processes on steep slopes, as well as in interpreting old lava–debris sequences found in other steep-sided volcanoes subject to effusive activity.

Keywords Lava flow field · Morphology · Tumuli · Lava tubes · Effusion rate · Rheology · Stromboli volcano

Editorial responsibility: A. Woods

L. Lodato (✉) · L. Spampinato · S. Calvari
Istituto Nazionale di Geofisica e
Vulcanologia–Sezione di Catania,
Piazza Roma 2,
95123 Catania, Italy
e-mail: lodato@ct.ingv.it

L. Spampinato
Department of Geography, University of Cambridge,
Cambridge, UK

A. Harris · M. Patrick
HIGP/SOEST, University of Hawai'i,
Honolulu, HI, USA

J. Dehn
Alaska Volcano Observatory, Geophysical Institute,
University of Alaska Fairbanks,
Fairbanks, USA

Introduction

On 28 December 2002, a new effusive eruption started at Stromboli volcano (Aeolian Islands, Italy) that continued until 22 July 2003. A detailed account of the chronology of the eruption has been given by Calvari et al. (2005). Thus, we summarize only the elements of the chronology that are essential for understanding the analysis of the lava flow field evolution presented in this study. Effusive vents became established at the base of the NE crater or Crater 1 and within the Sciara del Fuoco (Fig. 1). Lava flows extended down the Sciara del Fuoco, where an average slope of 35° was maintained along the 1.7-km flow course

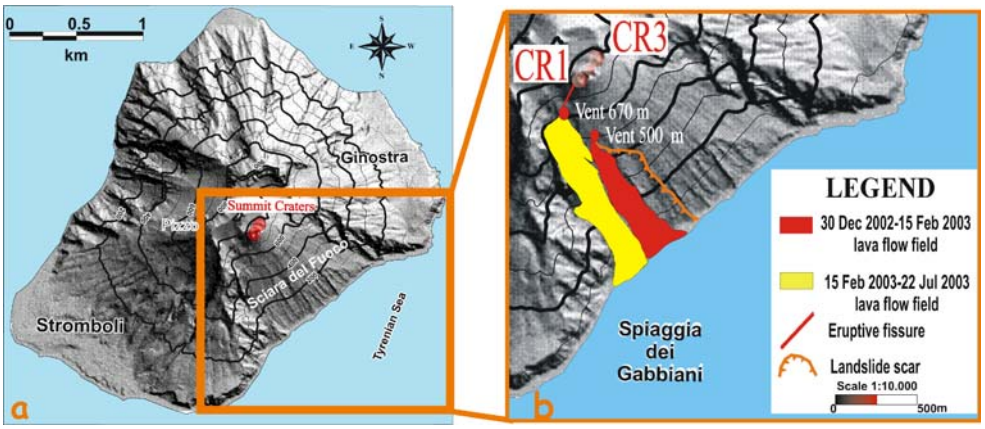

Fig. 1 Map of Stromboli, showing **a** the flank effected by the 2002–2003 lava flows, and **b** the 30 December 2002 landslide scars (*yellow lines*) and the lava flow fields on the Sciara del Fuoco fed by the 670- and 500-m vents. North is at the *bottom*, *CR1* is the NE crater, and *C3* is the SW crater. Adapted from Calvari et al. (2005)

between the erupting vents and the coast. Subsequently, two main lava flow fields were emplaced. The first was fed by a vent at 500 m elevation between 30 December 2002 and 15 February 2003, the second was mostly emplaced between 15 February and 22 July 2003 from a vent at 670 m (Calvari et al. 2005; Fig. 1). Both flow fields developed either totally or partially on the extremely steep slopes of the Sciara del Fuoco (Fig. 1), resulting in distinctive flow field morphologies.

The development of these flow fields gave us an excellent opportunity to examine the morphology and evolution of flow fields emplaced on inclined surfaces. Although numerous studies have described basaltic lava flow field morphologies and emplacement processes on flat-to-gently sloping surfaces (e.g., Kilburn and Lopes 1988; Hon et al. 1994; Peterson et al. 1994), only a few have described these processes for such extreme slopes (Lyell 1858; Borgia et al. 1983; Cigolini et al. 1984). During the 2002–2003 Stromboli eruption, regular (daily) monitoring with hand-held, and sometimes tripod mounted, thermal imagers [Forward Looking InfraRed Radiometer (FLIR)] and digital cameras provided a data set from which the flow field morphology and evolution could be examined (Calvari et al. 2005). In addition, precise feature locations and dimensions were obtained using laser ranger finders and triangulation in the FLIR and digital camera images, where all images were geo-located using GPS and ground control points (Harris et al. 2005). In this study, we use these data to detail the morphology and evolution of the flow field, and relate this evolution to quantitative parameters such as effusion rate, number of active vents, flow length, and number of active flows. In doing this, we define the characteristics of basaltic flow fields emplaced on steep slopes.

Flows were extremely unstable and suffered from almost constant flow front collapses to feed hot grain flows extending down-slope from the flow fronts. Larger rock falls from the lava flow field and collapse scars resulting from the December 30 flank failure (Bonaccorso et al. 2003; Pino et al. 2004) frequently sent larger blocks rolling and bouncing down the Sciara at high velocities, often landing in the sea up to 50 m off shore. In addition, the flow field was emplaced at the base of 100–150 m high cliffs. These factors made close approach to the flow field a hazardous and difficult undertaking. In such cases, feature analysis by means of hand-held remote sensing techniques is an extremely powerful and attractive tool, facilitating safe and efficient monitoring and analysis of developing flow features. The FLIR data also allow numerous quantitative flow field parameters to be extracted, such as number of active vents, number of flows, flow length, heat loss, and effusion rates. The methodology used to calculate effusion rate from both the FLIR and satellite data, as well as the derived effusion rates, error, and problems are given in Calvari et al. (2005) and Harris et al. (2005). The full effusion rate data set from Calvari et al. (2005) is given in Fig. 2a, with a 7-point running mean applied to smooth the data.

Previous effusive eruptions at Stromboli

Although Stromboli is associated with persistent moderately explosive (strombolian) activity, lava flows have been a relatively common feature of Stromboli's activity. Since the formation of the Sciara del Fuoco during a major collapse event affecting the NW sector of the volcano ~5 ka (Kokelaar and Romagnoli 1995), lava flow activity has occurred largely within the Sciara. Over historical times, all lava flow activity has been confined totally to the Sciara by the high cliffs surrounding the 2-km wide collapse scar. This has effectively protected the rest of the island from lava inundation. Lava flow activity during the last ~5,000 years, combined with the persistent ejection of material onto the Sciara, has been responsible for steady filling of the 0.97–1.81 km^3 collapse scar with 0.32–1.16 km^3 of material (Kokelaar and Romagnoli 1995).

Small lava flows and ponds have also been frequently observed within the active summit crater complex, i.e., the

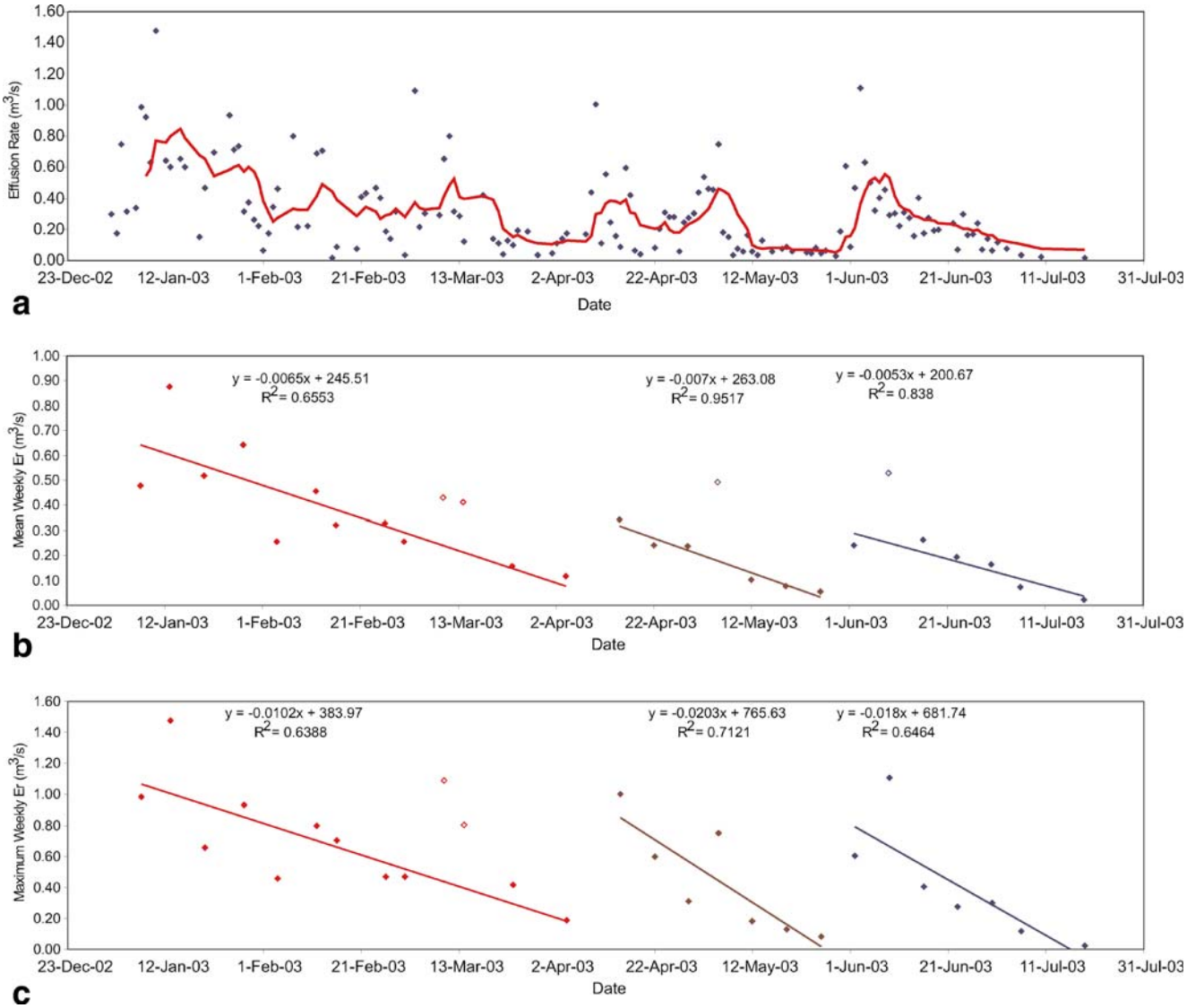

Fig. 2 **a** Total effusion rate data set from Calvari et al. (2005) with a seven-point running mean (*red line*). **b** Average weekly effusion rate and **c** maximum effusion rate in each week showing three periods of linear decay

crater terrace. These, however, are extremely minor effusive events of limited extent, remaining within the confines of the crater terrace. A small pahoehoe pad was emplaced within the crater terrace sometime between June 2000 and April 2001, for example, attaining dimensions of just 50×10 m and a bulk volume of ≤500 m^3. We distinguish major effusive events as being those that result in emplacement of lava onto Sciara, i.e., beyond the confines of the crater terrace, and involving the eruption of significant lava volumes (>10^5 m^3) during persistent effusive activity lasting days-to-months. In addition, vent locations differ between minor and major effusive events. Minor effusive events are fed by the persistently active strombolian vents within the crater terrace, and may be viewed as overflow of the lava from the open vents during times when the magma levels are particularly high in the central column. In contrast, the new lateral vents that establish on the Sciara to feed major effusive events remain active only for the duration of the effusive events. These events thus result from short-lived breaching or tapping of the central magma column somewhere below the level of the summit vents.

Before December 28, 2002, the most recent major effusive event was that of December 1985 to April 1986 (De Fino et al. 1988), an event that had marked similarities with the 2002–2003 eruption. The 1985–1986 eruption began on 6 December 1985, and continued for 141 days. Like the 2002–2003 eruption, effusive activity was fed by a vent on the NE flank of the NE crater (or Crater 1) at an elevation of 670 m, a location identical to the vent location

for the 2002–2003 eruption. Initially, relatively high, but variable, effusion rates (4–5 m^3/s) fed lava flow to the sea (De Fino et al. 1988). Thereafter, effusion rate gradually diminished, being no more than 0.5 m^3/s by April 16 and resulting in a 5–6×10^6 m^3 flow field (De Fino et al. 1988; Harris et al. 2000), a value that gives a mean output rate of 0.4–0.5 m^3/s. Ephemeral vents were active between the 630 and 580 m elevation and were distributed across a platform to the NE of the crater terrace and at the head of the Sciara del Fuoco building an ~20-m thick lava platform or shield in this location. After 25 December 1985, lava flows from these vents did not extend below the 450-m elevation, building a compound ′a′a flow field covering the eastern sector of the Sciara (De Fino et al. 1988).

Chronology of the effusive activity during the 2002–2003 Stromboli eruption

At 18:30 (all times are local) on 28 December 2002, a NE–SW trending eruptive fissure opened on the northeast flank of NE crater (CR1 in Fig. 1; Calvari et al. 2005). The

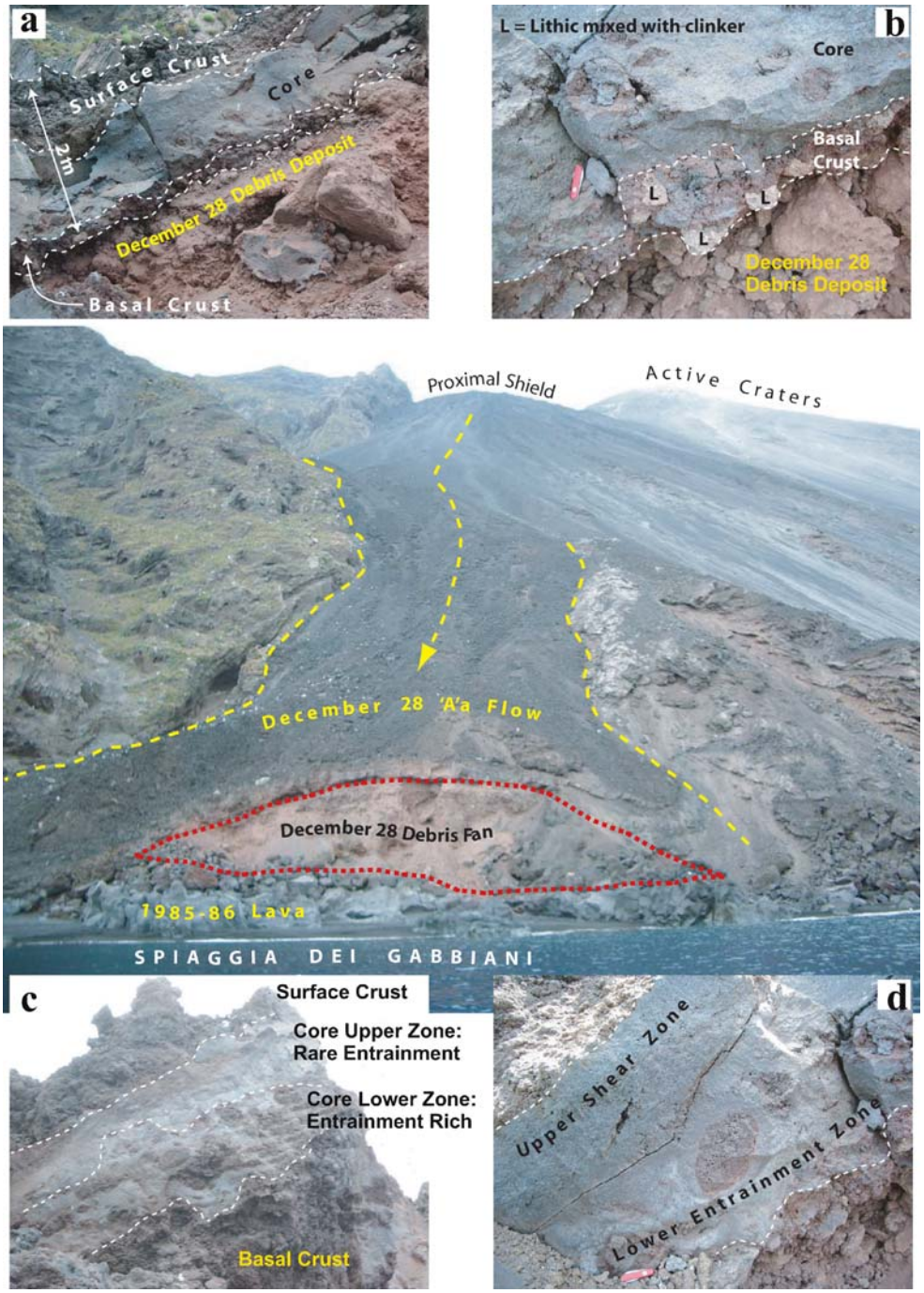

Fig. 3 The 28 December ′a′a lava flow (*eastern arm*), view from North, with insets showing **a** flow section comprising surface clinker, core, and thin basal clinker, **b** lithic mixing in the thin basal crust, **c** entrainment-rich lower core zone, and **d** shearing in the upper core zone with entrainment in the shear-free lower core zone

fissure fed a fast-moving lava flow that tapped lava previously ponded within NE crater and the shallow plumbing system. This ′a′a flow moved over a hot avalanche deposit emplaced during the initial phase of the eruption (Fig. 3), extending in two branches down the eastern and western margins of the 1985–1986 flow field, reaching the sea at the Spiaggia dei Gabbiani (Fig. 3). The first flows covered the 1.7−km distance from the vent to the coast in less than 30 min (Calvari et al. 2005).

After the initial activity of 28 December, there was a short hiatus of ~22 h, with no observed lava flow activity until the afternoon of 29 December. By the morning of 30 December, a new effusive vent had established at the 670−m elevation (Calvari et al. 2005). A second vent formed after midday at the 500-m elevation after a major landslide (Bonaccorso et al. 2003). This vent was located within the largest landslide scar and fed a lava flow that reached the sea. Effusive activity from the 500-m vent persisted until 15 February 2003 to build a compound lava flow field in the central section of the Sciara del Fuoco (Fig. 1). Lava flow from the 670-m vent was initially sporadic, where short, slow moving lava flows were active for periods lasting from a few hours to a few days during January and February (Calvari et al. 2005). After the closure of the 500-m vent on 15 February, however, effusion from the 670-m vent became persistent, feeding a compound lava flow field on the eastern side of the Sciara del Fuoco (Fig. 1).

Although explosive activity was generally absent from the summit craters during the effusive eruption (Ripepe et al. 2004, 2005), a major explosive event occurred on 5 April (Calvari et al. 2006). This event, although completely covering the upper flow field (above the 500-m elevation) with a carpet of pyroclastics, did not interrupt the lava flow activity. As reported in this study, a decline in effusion rate and flow length was noted after 6–7 June. This represented the onset of a final period of extremely low effusion rate flow that heralded the total cessation of effusive activity on 21–22 July. During the 175 day eruption, $\sim 13 \times 10^6$ m^3 of vesicular lava was erupted (Calvari et al. 2005), giving a time averaged bulk mean output rate of $0.9\,m^3/s$.

The 28 December lava flow: ′a′a emplacement on a steep slope

The first lava flow to reach the sea on 28 December extended the ~1.7 km distance from the vent to the coast in 10–20 min. This gives a time averaged flow front velocity of 4–9 km/h. One flow arm moved down the eastern edge of the Sciara del Fuoco to spread across the beach at Spiaggia dei Gabbiani to build a lava delta at the sea entry with a flow front width of ~70 m (Fig. 3). As of June 2004, this flow was well exposed at the coast where it mantled the debris deposits of December 28. Here, the flow consisted of an ~2-m thick single ′a′a flow unit, with little variation in thickness across the entire flow front (Fig. 3). The surface consisted of 60–85 cm thickness of ′a′a clinker overlying an ~1-m thickness of massive core (Fig. 3a). The basal clinker was much thinner and, in places, was completely absent, with a typical thickness of 10–40 cm. The basal clinker was mixed with accidental lithics of dense, nonspinose (sometimes fumarolically altered) angular chunks (Fig. 3b). The core displayed a high incidence of entrained clinker. In places, this comprised around 50% of the core volume, but was typically concentrated in the lower half of the core (Fig. 3c, d). The core was also characterized by shearing only in its upper half, with a complete absence of shear structures in the lower half (Fig. 3d).

These features are consistent with sliding flow front advance. Although ′a′a flows are typically associated with a rolling, caterpillar-track-like mode of advance, the steep, unconsolidated slope, comprising largely of rounded blocks and ash, on which this ′a′a flow was emplaced, caused it to slide. During such sliding, the basal clinker and underlying material behaves like marbles, rolling beneath the flow. This explains the mixing of the thin basal clinker with the underlying material and the high volumes of entrained material, where rolling increases the ability of basal material to penetrate and enter the soft-core base. In addition, clinker spalling from the advancing flow front continued to tumble down the steep slope and away from the flow front. Usually, such clinker gathers at the flow front to be overridden by the advancing flow or rolls beneath the flow to contribute to a significant basal clinker that characterizes the classic ′a′a section (Kilburn and Guest 1994). Such material would have been unavailable in this case, thus explaining the lack of basal crust. The sliding action would have decreased the advance time of the flow front over that expected under normal (classic, gentle slope) flow conditions.

Lava flow field morphology: spatial classification and characteristic features

Flow field morphologies were strongly dependent upon underlying slope. We divide the flow field into four zones; each of which has characteristic slopes and morphologies. Before 5 April 2003, four morphological zones were apparent (Fig. 4, Table 1):

(1) *Low gradient (0–15°) proximal zone* (Fig. 4a). This zone developed within the upper flow field, i.e., between 670 and 600 m a.s.l. and around the main

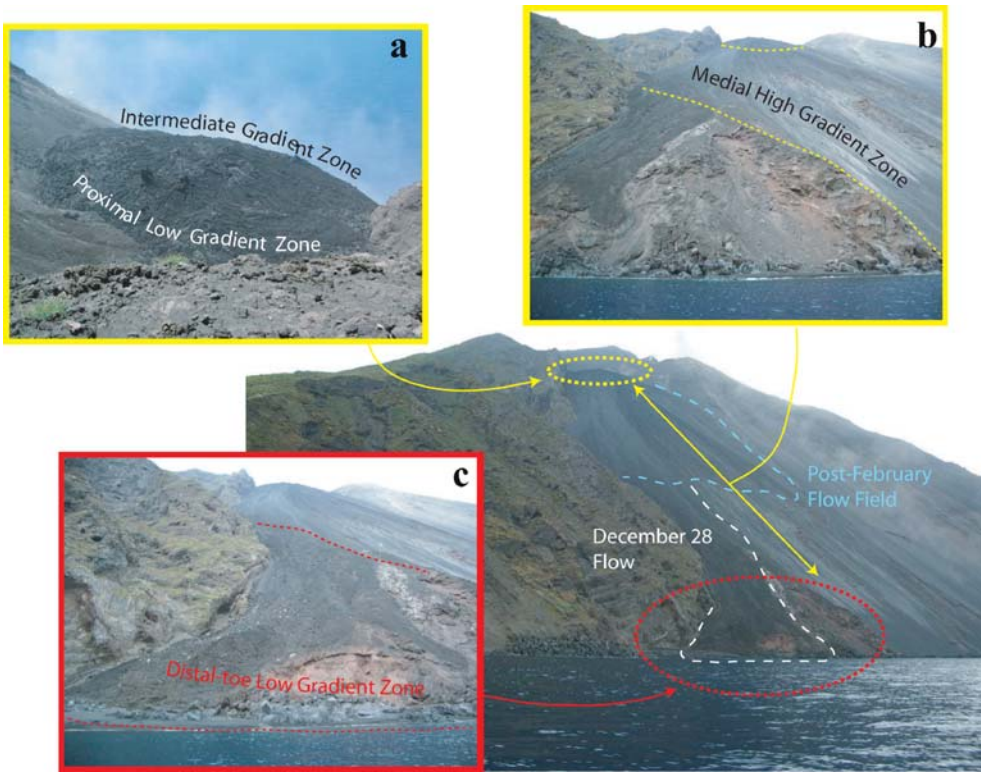

Fig. 4 The lava flow field fed by the 670-m elevation vent, showing details of **a** the proximal and intermediate gradient zone, **b** the medial high gradient zone, and **c** the distal-toe low gradient zone. View is from north

vents at the base of the NE crater. Before the eruption, this zone was characterized by a 210-m diameter bench containing the proximal section of the 1985–1986 flow field. During the 2002–2003 eruption, frequent emission of short flows, as well as inflation, built a low gradient shield composed of a compound flow field within this zone (Fig. 5a 1–4). As described later, this feature resulted from the coalescence of a series of tumuli and their resultant flows. Although ′a′a was the dominant lava flow morphology, this was the only zone within which pahoehoe sheet flow was observed, resulting in localized units comprising pahoehoe slabs with spiny surfaces of the Etnean pahoehoe type (Polacci and Papale 1997).

(2) *Intermediate gradient (15–30°) medial zone* (Fig. 4a). The topographic bench within which the proximal shield developed was bounded to the NE, SW, and SE by cliffs rising to an altitude of 750–900 m. These cliffs thus limited flow advance in these directions and caused flows to pile up. However, due to the presence of the eruptive fissure, a master tube soon developed across the lava shield. The shelf was open to the NW (Fig. 5a, 5), and here, flows were able to extend onto and down the steep (30–35°) slopes of the Sciara del Fuoco. Initially, flows moving away from the proximal zone encountered intermediate (15–30°) slopes across a 40- to 60-m wide zone between the 600- and 580-m elevations. Across this zone, channels and tubes

Table 1 Summary of flow field morphological zones and their characteristic features

Zone	Elevation (m a.s.l.)	Slope (degrees)	Associated features	Figure
Low gradient, proximal	670–600	0–15	Tumuli; tumuli-fed ephemeral vents; sheet-flow (slabby-spiney pahoehoe); ′a′a; tubes, skylights; tube-fed flow	4a
Intermediate gradient, medial	600–580	15–30	Classical channels; tubes; tube-fed ephemeral vents; ′a′a with central plug flow; channels with excavated levees	4a
High gradient, medial–distal	<580	>30	Tube-fed ephemeral vents; tubes; skylights; skylight-fed flow; channels with excavated levees; ′a′a with central plug flow; buried channels; grain flow fed by flow front; collapse; debris field	4b
Low gradient, distal (toe)	<30	5–15	Classical channels; ′a′a with central plug flow; dispersed flow; sea-entry flow; lava deltas	4c

developed. In effect, it represented a zone of transport, linking the proximal source zone (shield) with the distal lava flows. Tubes opening in this zone fed short-lived channels (Fig. 5a, 6 and 7), within which flow was characterized by central plugs composed of slabs of cooler crust, bounded by higher temperature marginal shear zones of ′a′a clinker. Interesting features commonly observed in this zone were excavated debris levees (Calvari et al. 2005). These formed by lava flows mechanically excavating a channel within the loose, unconsolidated material over which they extended, causing channels bounded by excavated levees (Fig. 5a, 5).

(3) *High gradient (>30°) medial–distal zone* (Fig. 4b). Between the lower edge of the intermediate zone and the sea, the topography was characterized by slopes in excess of 30°. Tubes extending into this zone opened to feed tube-fed ephemeral vents linked back to the distal shield by the tube. In addition, short lived ′a′a flows occasionally spilled out of skylights to form short overflows, often extending in pairs to form a moustache-like flow-plan (Fig. 5b, c). All channels within this zone displayed the excavated form, within which ′a′a bounded plug flow was apparent (Fig. 5d). As in the intermediate gradient zone, the excavated channel form was a result of the fine-grained deposits that covered this zone. In addition, the steep slopes contributed to flow front and levee instability, such that collapse was nearly continuous (Fig. 5d, e). These fed debris avalanches and grain flows down the Sciara del Fuoco to the sea. These in turn contributed to the fine-grained substrate that favored excavation. Finally, collapses from higher on the flow field would occasionally bury lengths of active channel, contributing to tube formation. We note that this mode of tube formation is different to slower processes typically associated with tube formation (Swanson 1973; Peterson et al. 1994; Calvari and Pinkerton 1998, 1999), the burial being a sudden event.

(4) *Low gradient (5–15°) distal–toe zone* (Fig. 4c). Two low gradient zones were apparent in the distal section. The first was located on the eastern edge of the Sciara del Fuoco extending from the 300-m elevation to the sea at Spiaggia dei Gabbiani (Fig. 4). The second was located 500 m west from the eastern edge of the Sciara del Fuoco, and extended from the 30-m elevation to the sea (Fig. 5a, b and c). Across both of these locations, slopes were between 5 and 15°. These zones were characterized by lava flow (Fig. 5a, c) in classical (constructional) channels (Lipman and Banks 1987). However, channels often fed distal zones of dispersed ′a′a flow. In addition, because of the proximity to the sea, flows extending to the coast resulted in sea entry and the construction of lava deltas (Fig. 5b, c).

Flow field development I: shield construction in the proximal zone

After the shut down of activity at the 500-m vent on 15 February, effusion at the 670-m vent became stable, with lava effusion persisting until the end of the eruption on 22 July (Fig. 2a). Thus, the bench at the base of the NE crater became the locus of activity, such that a complex, compound lava field developed over the vents. This piling up of flows around the vent zone resulted in the construction of an ~50-m thick lava shield at the head of the flow field, that became the source of all flow into the medial and distal flow field sections (Fig. 5a, 1–4). However, construction of the shield was not simply the result of piling one lava flow on top of another, but construction resulted from a number of exogenous and endogenous flow field processes. Namely, endogenous growth resulted in inflation and tumuli construction, where tumuli also became coated in a series of lava flows emplaced in an exogenous style from vents on and around the parent tumuli. In addition, the extension of tubes away from various tumuli fed new ephemeral vents that marked the tube exits. At such locations, further tumuli developed. As a result, lava distribution became spread around the proximal zone to build a broad shield of coalesced tumuli, lava flows, and hornito's linked by a complex network of tubes (Fig. 5a, 1–4).

Shield development before 5 April

Before 15 February, sporadic lava output from the 670-m elevation vent fed numerous short lava flows, to form a small compound lava flow field. Flows extending westwards moved onto the shallow slopes of the low gradient proximal zone (Fig. 5a), and developed sheet-like surface morphologies. However, those extending northwards onto the Sciara del Fuoco moved into the medial, high gradient zone where ′a′a surface morphology's excavated debris levees and hot avalanches from failing and crumbling flow fronts developed (Fig. 5d, e).

This activity generated the first of a series of dome-like features within the vent region. Because these features were formed by endogenous growth resulting from lava injection and sheet flow inflation, as well as piling up of surface flows, in this study, we term them tumuli after earlier classifications (Walker 1991; Rossi and Gudmundsson 1996; Duncan et al. 2004). Our terminology is summarized

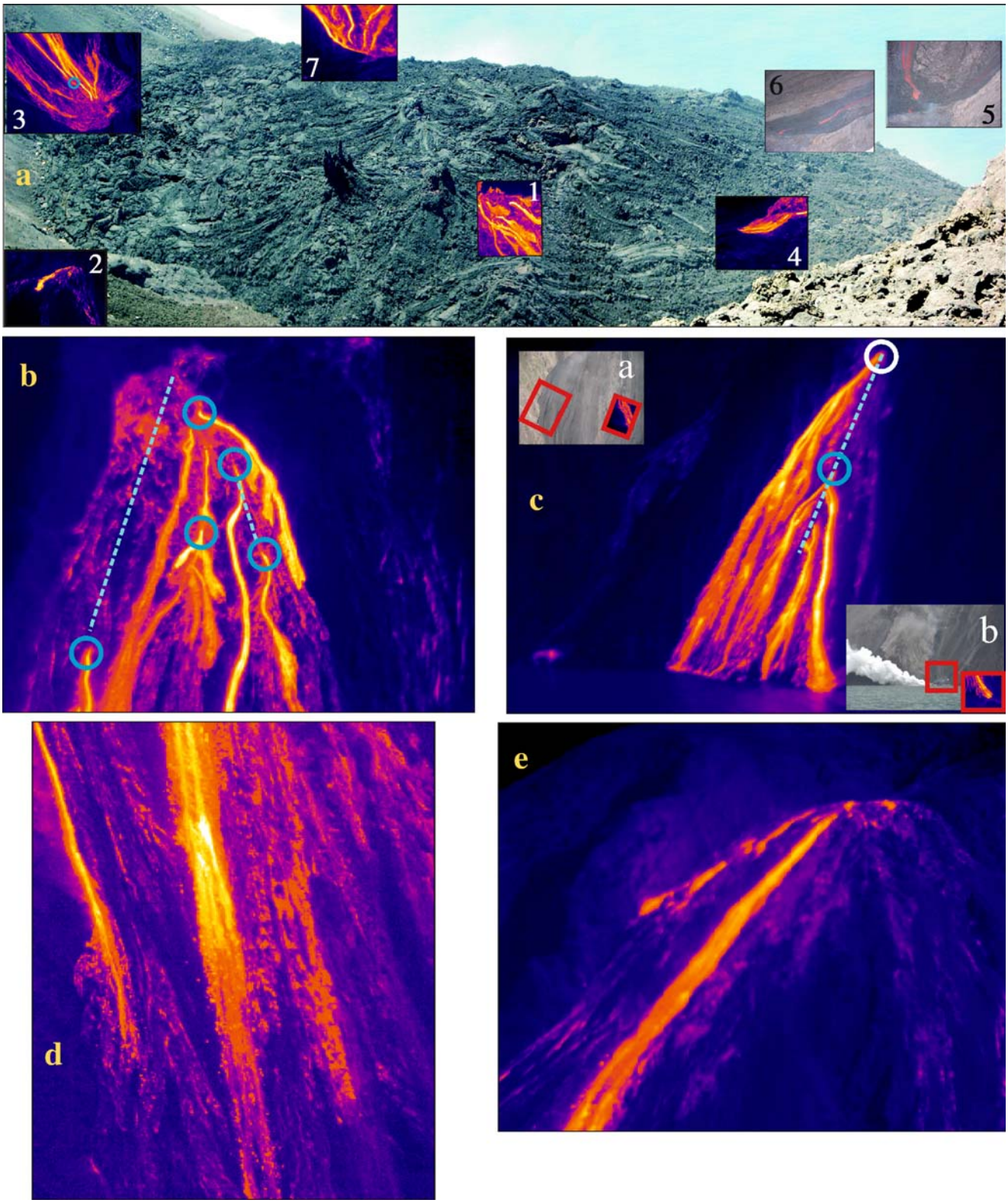

in Fig. 6. By 15 February, the first tumulus was just distinguishable and represented in the terminology of Duncan et al. (2004), a primary focal tumulus (Tumulus A, TA), being located over and directly fed by the source vent. It subsequently became linked to, and fed, subsequent satellite tumuli (TB-TD) by tube development (Fig. 6).

Although activity was initially focused at TA, by 16 February, the prime source of surface activity had shifted

◀ **Fig. 5** **a** View from SE of the proximal low gradient zone of the lava flow field fed by the 670-m elevation vent, with details of structures revealed by thermal images inset: (*1*) ephemeral vents, (*2*) sheet flow, (*3*) lava tubes and skylight (*blue circle*), and (*4*) overflows from skylights. In the thermal images, *yellow* reveals the hot end of the thermal scale, *blue* is cold. Structures observed in the intermediate gradient zone of the lava flow field fed by the 670-m vent are also inset in **a** showing: (*5*) channels with excavated debris levees (Calvari et al. 2005), (*6*) lava tubes, and (*7*) ephemeral vents. Structures observed in the high gradient zone of the lava flow field fed by the 670- and 500-m vents: **5b** tube-fed ephemeral vents (*circle*), lava tubes (*dashed line*) and flows fed by skylights; **5c** ephemeral vent (*white circle*) and skylight (*blue circle*) connected by lava tube; **5d** grain flows fed by flow front collapse; **5e** lava channels bounded by excavated debris levees (Calvari et al. 2005). Also shown are classical channels observed on 10 April 2003 in the distal low gradient zone of the lava flow field fed by the 670-m vent (**5c**, a). These were located at the eastern margin of the lava flow field on the Sciara del Fuoco. **5c** (b) shows the sea-entry situation on 31 December 2002 in the distal low gradient zone on the western side of the lava flow field fed by the 500-m vent: note steam plume at entry and lava delta apparent in thermal image

20–30 m to the west due to the development of a tube extending from the base of TA and aligned along the depression associated with the NE trending fissures in this location. By 21 February, the lava tube had become stable and surface activity at TA died out. However, a persistent thermal anomaly at TA revealed that lava continued to flow into and through it, thus confirming its role as the primary focal tumulus to which all others were linked. Thereafter, the development of tumuli and tubes became a characteristic of the low gradient proximal zone, so that a family of linked tumuli developed at the head of the system (Fig. 6).

On 16 February, several ephemeral vents were apparent at the exit of the tube extending from TA. These, in turn fed, a number of surface lava flows. These vents were located at a break in slope within the proximal zone. Thus, the tube was stable over the relatively gentle and constant up-flow

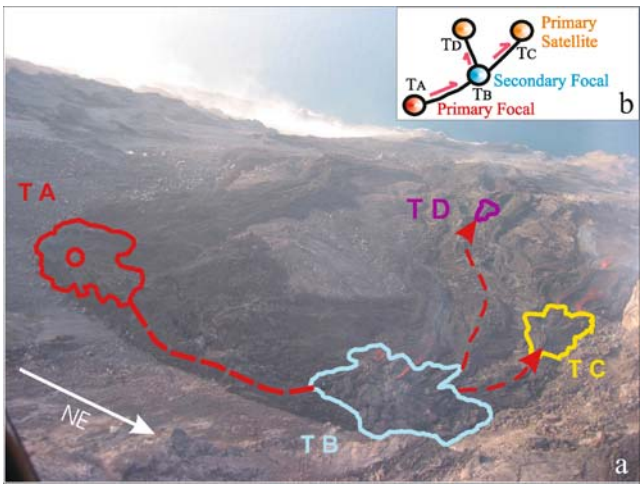

Fig. 6 **a** Photo taken on 18 March 2003 revealing the four main tumuli of January–March, and **b** sketch showing schematic of tube–tumuli complex hierarchy before the 5 April 2003 event

gradients, but fed flow at the point at which an increase in the underlying gradient occurred. Further downflow, the gradient declined once more, causing flows to pile up at this location. By 18 February, these flows had already generated a second focal tumulus structure (Tumulus B, TB) at about 630 m elevation. As shown in Fig. 6, this topographic configuration of tube-linked-tumuli was a characteristic of the proximal zone. Within this, while tubes became characteristic of zones across which slopes were constant, tumuli and breakouts marked zones where slopes were changing (Mattox et al. 1993; Calvari and Pinkerton 1998).

In the next days, TB formed three single lava flows, two moved towards Sciara del Fuoco, and the third westwards. By 20 February, this third flow constituted a 10-m long lava tube that extended between 630 and 600 m a.s.l. The tube fed five ephemeral vents that on 22 February created a third tumulus structure (Tumulus C, TC) at a break of slope around the 600-m elevation. This satellite tumulus was linked, via a complex tube system, to TB (Fig. 6). TA, by now, was a somewhat relict structure through which lava simply passed, effectively representing a construct that formed over the main vent during the opening phase of the eruption. TB, however, became the most active feature, feeding flows to subsequent satellite tumuli.

The construction of TC signaled a further development in the growth of the proximal section flow field. During the days after 22 February, TC fed flows from numerous ephemeral vents (Fig. 7a). However, between 27 February and 9 March, its activity gradually decreased. Surface activity at TB had already began to wane by 22 February, with activity dying out rapidly such that this structure did not feed any surface flows between 23 February and 3 March. Thereafter, surface activity at both tumuli was highly variable, with the number of active vents varying between 0 and 10 (Fig. 7a).

On 17 March, a fourth satellite tumulus (Tumulus D, TD) linked to TB established at the 580-m elevation, a location that marked another break in slope and a tube exit (Fig. 6). At first, TD was extremely active, supporting nine ephemeral vents, but soon became inactive after this initial peak, remaining inactive until 28 March when it turned on again (Fig. 7a). Thereafter, tumuli TB, TC, and TD displayed variable levels of activity until 5 April (Fig. 7a).

Shield development after 5 April

By the morning of 5 April, just before the paroxysmal explosion, TB and TC had just one ephemeral vent each, while TD had two (Fig. 7a). The paroxysm itself covered the proximal shield with an ~10-m thick carpet of pumice (Calvari et al. 2006), causing a significant change in the surface morphology of the upper flow field. Mainly, the event (1) buried the preexisting shield, and (2) extended the

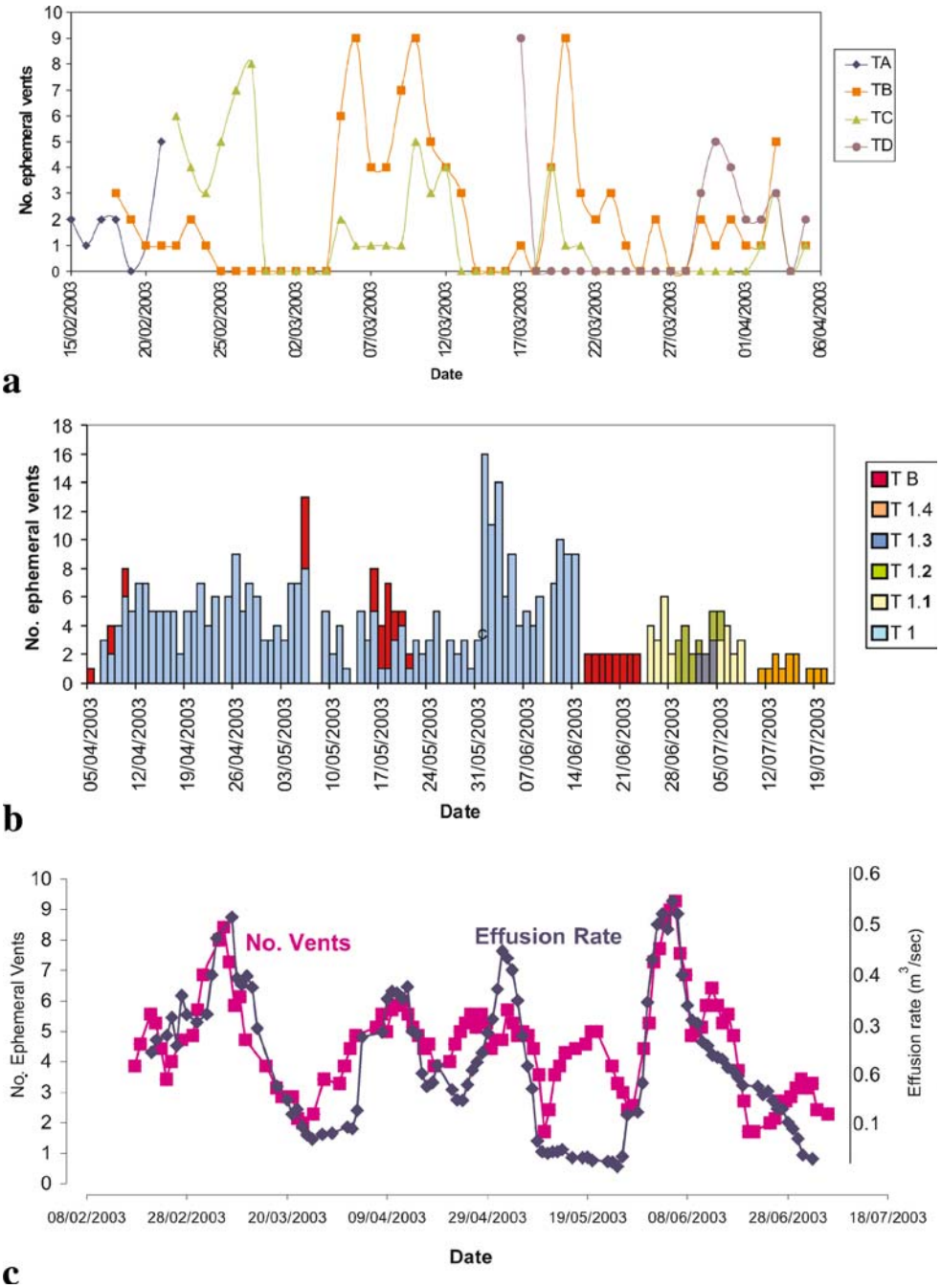

Fig. 7 **a** Number of ephemeral vents fed by each tumulus up to 5 April 2003. **b** Number of ephemeral vents fed by tumuli TB and T1, and by ephemeral tumuli T1.1, T1.2, T1.3, and T1.4 after the 5 April explosive event. **c** Correlation between smoothed (seven-point running mean) data for the number of active ephemeral vents and effusion rate. Effusion rate values are from Calvari et al. (2005)

proximal bench ~10 m in the direction of the Sciara. This caused the contact between the proximal low and intermediate slope zones to migrate downflow. Morphologically, the effects of the paroxysm were felt over the entire flow field, where pumice fall filled depressions between individual lava flows across whole field.

Lava effusion was completely unaffected by the April 5 event. Less than 2 h after the explosion, new lava flows emerged from beneath the pumice carpet at the new break in slope at the head of the Sciara (Fig. 8a). These flows had three distinct emission points, each of which could be directly linked to the three buried tumuli (TB, TC, and TD) (Fig. 8b). This indicates that the tumuli continued to be active immediately after the 5 April explosive event, with lava moving from them beneath the tephra blanket forming lava tubes within the debris by forcing the carpet upwards through hydrostatic pressure and/or through excavation (Fig. 8c). Certainly, the material was of low density and poorly consolidated, facilitating both uplift and excavation in the 2 h after the explosion as new flows moved away from the tumuli.

By 7 April, the three vents at the new break-of-slope vents had already generated a new group of tumuli. These were Tumuli 1 (T1), 2 (T2), and 3 (T3) (Fig. 8a, b).

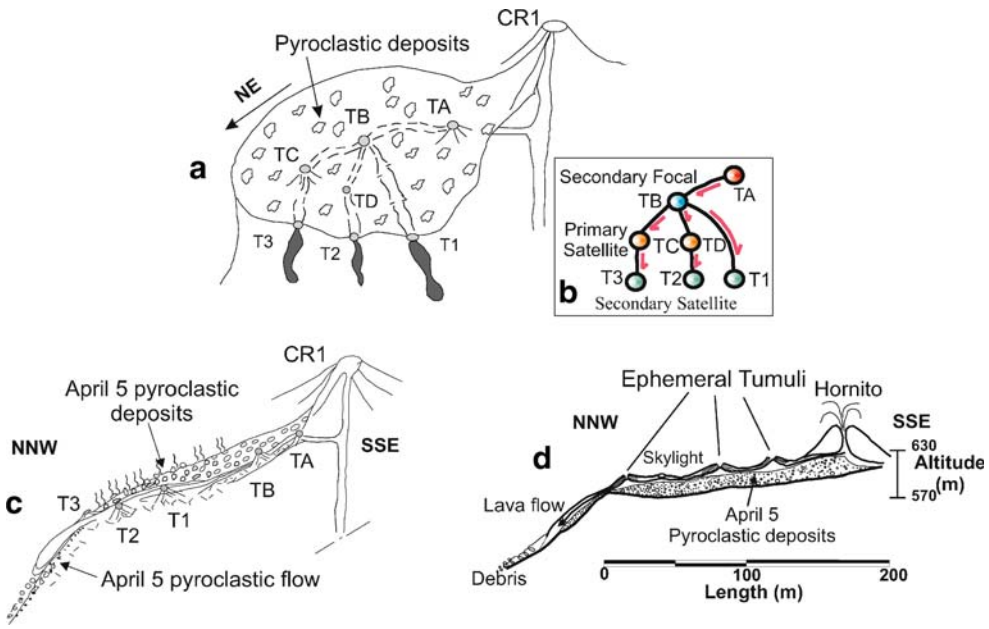

Fig. 8 **a** NNW–SSE section of the proximal lava shield indicating spatial relationships between the 5 April pyroclastic deposits, active tumuli, and the active lava flows. **b** Schematic plan view showing the position of tumuli the tube–based links between them. **c** Sketch showing spatial relationships between tumuli and the 5 April deposits. **d** Sketch showing a NNW–SSE section through the proximal lava shield between tumuli T1 and TB indicating spatial relationships between the 5 April pyroclastic deposits and the active lava field emplaced after this event, with location of skylights, hornito, and ephemeral tumuli (migrating upslope along the tube system) in the final stage of activity

These three satellite tumuli were respectively linked to tumuli TB, TD, and TC (Fig. 8b, c). Activity at T2 was short-lived, lasting only 2 days until 9 April. During its brief life, T2 was not particularly active, and its deactivation probably also marked the death of TD. Activity at T3 lasted until 11 April, when its supply died out, marking the termination of feeding not only at this tumulus, but also at the primary satellite tumulus TC to which it was linked (Fig. 8a, b).

Within the typical lava flow field evolution framework (Kilburn and Lopes 1988, 1991), the termination of activity at tumuli TD and TC signaled the onset of the phase of deactivation for the lava flow field. During such a phase, declining effusion rates are associated with a decrease in lava flow activity such that ephemeral vents begin to shut down and lava flow fronts begin to withdraw back towards the vent. This phase is characterized by an up-flow-field migration of the ephemeral tumuli themselves.

After the shut down of TD and TC, T1 became stable and produced lava flows that moved into the high gradient zone, sometimes extending as low as the 300-m elevation. The direct link between T1 and TB was clearly demonstrated by the simultaneous and linked behavior of the two tumuli on many occasions.

Tumulus B

After 8 April, activity at TB became characterized by degassing and spattering, such that by 18 April, a hornito had developed atop TB (Fig. 8d). Initially, a vent at the summit of this hornito fed short channelized lava flows that extended down the hornito flanks and onto the surface of TB to pond in small depressions. Beginning 2 May, a second hornito began to develop atop TB. However, during this time, ephemeral vent activity within the proximal shield was rare, represented only by brief periods of activity at TB, such as during 6 May (Fig. 7b). Although this activity only resulted in minor exogenous growth of TB, and thus of the proximal shield, significant endogenous growth was apparent from fracturing of the shield due to inflation. Such arcuate cracks began to open on 25 June, with a NE–SW orientation. These cracks crossed the active tube linking TB and T1, but did not cut or dislocate the integrity of this tube. Thus, the cracks did not penetrate the flow field to any great depth, being surface features associated with brittle failure of the surface crust during inflation.

Migration of tumulus 1 activity

Tumulus 1 displayed constant activity between April and June (Fig. 7b). The exact number of active vents, though, varied between 2 and 16, where variation could be linked to fluctuations in the effusion rate (Fig. 7b, c). After 16 June, a marked decline in effusion rate signaled the beginning of a migration in the location of activity, up the flow field towards TB. During this phase, of waning activity a series of ephemeral tumuli (T1.1–1.4, Fig. 7b) developed over the tube that linked TB with T1, each tumulus forming progressively further up-tube (Fig. 8d). As a result, a beaded feature developed, represented by a series of small tumuli aligned along the TB-T1 tube. These tumuli were mostly produced by exogenous processes, a result of piling up of a series of short lava flows fed by vents (or skylights) forming in the tube roof. In addition, a steady decline in the number of active vents was apparent during the final, very low effusion rate phase of the eruption (Fig. 7c).

Number of active vents, effusion rates, and correlations

Between February and March, the variation in the number of active vents showed an oscillating behavior, with three ~20 day long pulses in activity with peaks around 10 March, 13 April and 26 April–3 May, and troughs around 25 March, 19 April and 10 May (Fig. 7c). These can be related to oscillations in the effusion rate data of Calvari et al. (2005) and Harris et al. (2005). We observe well-defined effusion rate pulses with peaks and troughs occurring at the same time as those apparent in the vent number time series (Fig. 7c). However, a fourth pulse in the vent number time series during 10–26 May, peaking around 20 May, is not apparent in the effusion rate time series, which shows low and stable effusion rates at this time. However, a final increase in vent activity around 4 June is well correlated with a similar increase in effusion rate, before both parameters declined to generally low levels during the final month of the eruption (Fig. 7c).

Generally, the total number of vents active (ϖ) on the proximal shield shows a reasonable, positive, correlation with effusion rate (E_r) (Fig. 7c). Simply, an increase in effusion rate forces an increase in vent activity, where a pulse in supply to the active vent area could either cause increased effusion from a single vent and/or opening of new vents to cope with the increased flux. It appears that the latter scenario is reasonable. Considering the entire data set, we obtain $\varpi=9.6\ E_r+2.1$, $R^2=0.6$. The correlation before April 5 ($\varpi=11.6\ E_r+1.3$, $R^2=0.8$) is superior to that after the April 5 event ($\varpi=9.1\ E_r+2.4$, $R^2=0.6$).

Flow field development II: lava flow field construction in the medial–distal zone

After the initial high effusion rate emplacement of the 28 December ′a′a flow (Calvari et al. 2005), the medial–distal section of the flow field was fed at low, although variable, effusion rates (typically <1 m^3/s) (Fig. 9a) through channels and tubes extending from the proximal shield. The location, length, and number of active flows were also variable (Fig. 9b, c), with flow in any one location typically lasting for just a few days to hours. Repeated flow extension onto the Sciara del Fuoco thus built a complex, compound ′a′a flow field in the medial and distal zone. However, flow front and levee instability due to the steep slopes on which these flows developed led to almost constant crumbling and collapse, to feed rock falls and grain flow into the sea (Fig. 5d). As a result, after the eruption, there was little evidence of the medial–distal flow field, it all having been removed by collapse.

Fig. 9 **a** Effusion rate data smoothed using an seven-point-running [data from Calvari et al. (2005)]. **b** Smoothed lava flow length data (seven-point-running mean applied), and **c** number of active lava flows (seven-point-running mean is given). Each effusion rate pulse and eruption phase (*period*) is identified, along with the 5 April explosive event

Development of the 670-m vent flow field

During the second half of February effusive activity was relatively weak, and lava flows from the 670-m vent did not reach the sea, instead forming relatively short, single unit flows. The furthest extended flow fronts developed during 16 April, 1–3 May and 7–14 June, when lava channels fed a series of ′a′a flows which extended into the lower section of the Sciara. These flow fronts extended to relatively low elevations (100–150 m a.s.l.). Tube-fed ephemeral vents that opened between the 600- and 450-m elevations, and were linked to the main vent by a tube extending down the Sciara, fed these flows.

Typically, however, flow field construction was dominated by low effusion rate flow that formed tubes opening into channels on the medial–distal section of the flow field (typically above 300–450 m a.s.l.), to feed ′a′a flow. Thus, the typical active flow unit comprised five sections, listed from vent to toe (Fig. 10):

Section 1: Proximal section of tube-contained flow.
Section 2: Medial section of channel-contained flow.
Section 3: Distal section of unchannelized ′a′a flow.
Section 4: Toe section comprising a failing, crumbling flow front.
Section 5: Debris fan zone of lava debris avalanches and grain flow.

Each of these are marked by characteristic levels in the temperature profile taken down the center line of the flow (Fig. 10). After the 5 April paroxysm, lava effusion continued to build the flow field at a generally low rate. These fed numerous ′a′a flow units, with the same location and five-section morphology as before 5 April, each active for no more than a few hours to days at a time. With the death of tumuli T2 and T3 during 9–11 April, activity became concentrated at T1. This focused the entire flux at one vent. Before this time, the local effusion rate (E_{local}) from T1 was less than the total flux (E_r), the total flux being shared between three vents (T1, T2, and T3). Thus, after April 16, the total flux was erupted from T1 ($E_{local}=E_r$). The concentration of flux at one vent created the illusion that flow activity was increasing, however at this time effusion rates and flow lengths were in fact decreasing (Fig. 9a, b). This decrease in flux was no doubt responsible for the termination of activity at T2 and T3.

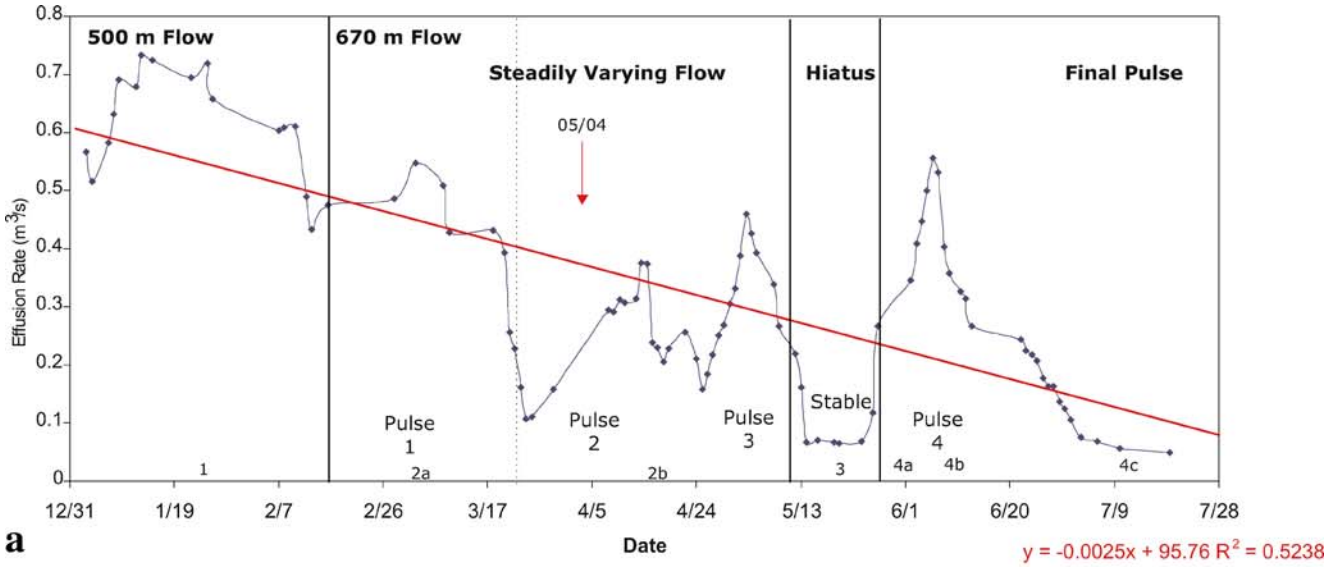
500 m Flow
670 m Flow
Steadily Varying Flow
Hiatus
Final Pulse
05/04
Effusion Rate (m3/s)
Pulse 1
Pulse 2
Pulse 3
Stable
Pulse 4
1
2a
2b
3
4a
4b
4c
12/31
1/19
2/7
2/26
3/17
4/5
4/24
5/13
6/1
6/20
7/9
7/28
Date
a
y = -0.0025x + 95.76 R2 = 0.5238

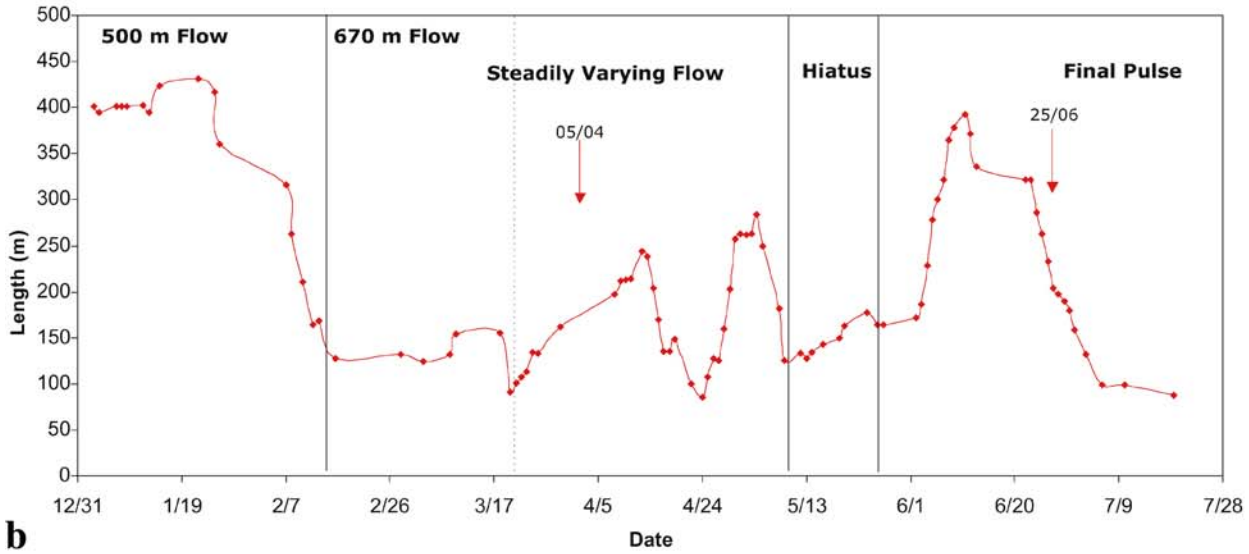
500 m Flow
670 m Flow
Steadily Varying Flow
Hiatus
Final Pulse
05/04
25/06
Length (m)
12/31
1/19
2/7
2/26
3/17
4/5
4/24
5/13
6/1
6/20
7/9
7/28
Date
b

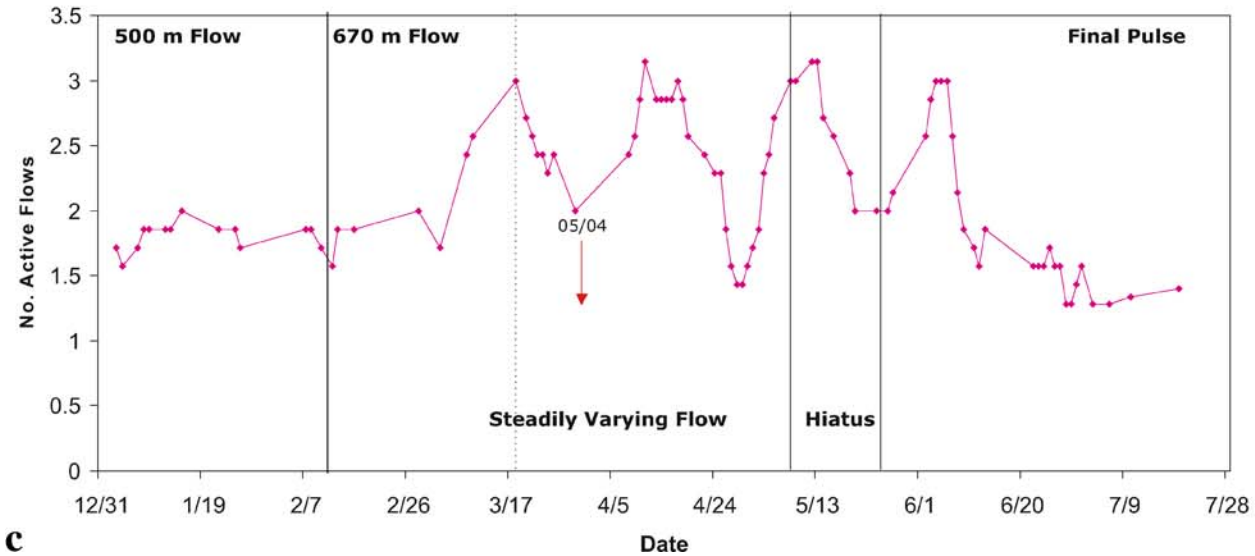
500 m Flow
670 m Flow
Final Pulse
05/04
Steadily Varying Flow
Hiatus
No. Active Flows
12/31
1/19
2/7
2/26
3/17
4/5
4/24
5/13
6/1
6/20
7/9
7/28
Date
c

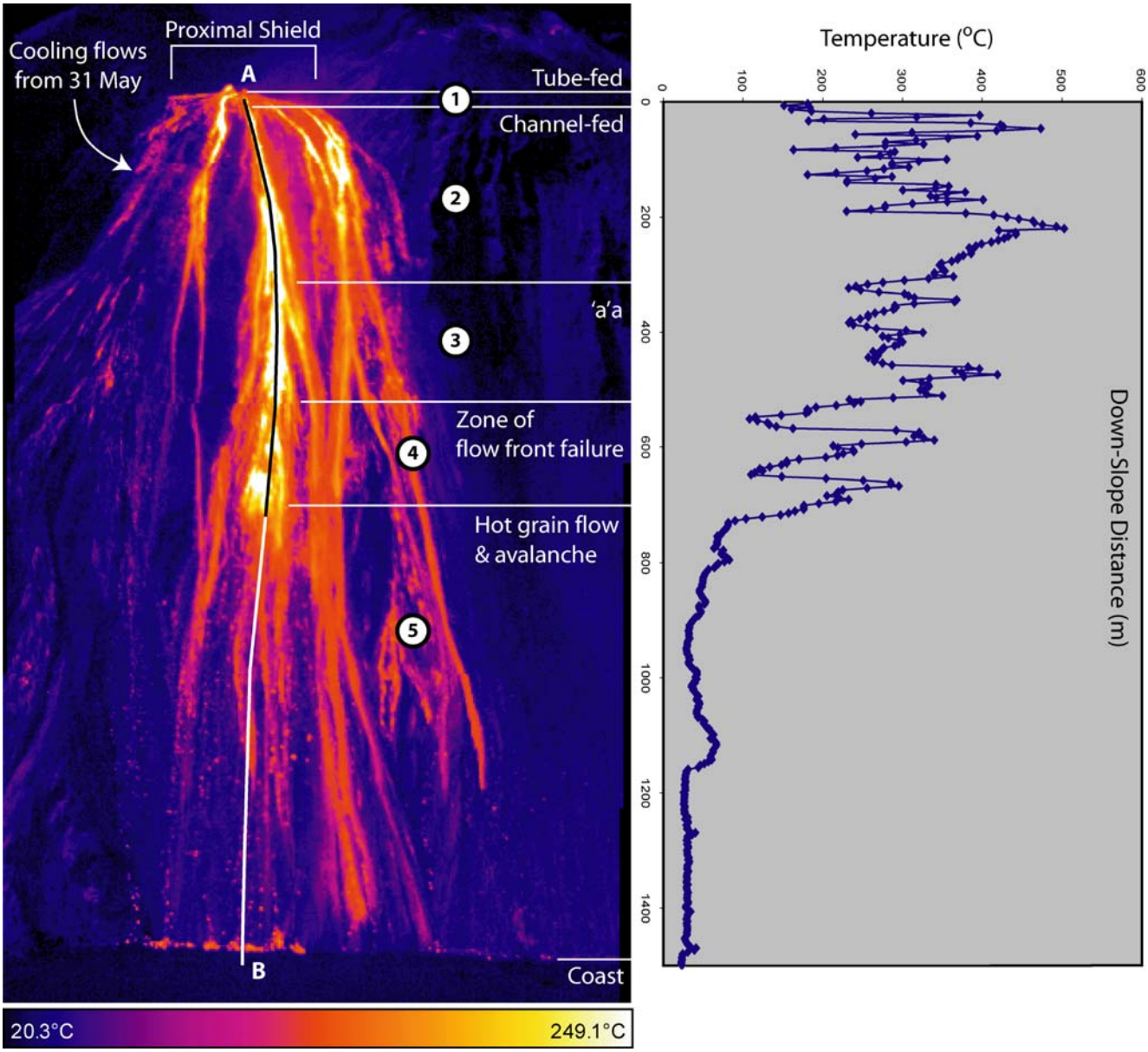

Fig. 10 Thermal image of the active lava flow field fed by the 670-m vent recorded on 6 June 2003 showing the five main morphological zones (*left*) with temperature profile (*right*) taken down the line marked **a**, **b**

The up-flow-field migration of T1 that began around 16 June was accompanied by a gradual decrease in flow length (Fig. 9b), and a retreat of the flow front positions to increasingly higher elevations, such that by 23 June lava flow activity was concentrated in the proximal and intermediate zones. Activity in the medial and distal sections of the flow field ceased by 9 July, all flow activity thereafter being confined to the proximal zone.

Effusion rate, flow length, and number of active flows

The effusion rate, flow length, and number of active flows data reveal systematic oscillations that are roughly synchronous across all data sets, but are best revealed by the effusion rate data (Fig. 9). After February 15, we identify four such oscillations or pulses (Table 2). The first three oscillations were roughly continuous; however, the final fluctuation followed an ~16-day long period of relatively stable effusion Fig. 9a.

Effusion rates

After the initial flow of 28 December, effusion rates were generally low (<1.3 m^3/s), with an average of 0.32 m^3/s (Table 3). However, effusion rates showed a general decaying trend during the eruption, declining from an initial high of 0.6–0.7 m^3/s during January to less than

Table 2 Main effusion rate pulses

Pulse	Starting day	Final day	Duration (days)	Peak E_r (m^3/s)	Peak date
1	28–Feb–03	25–Mar–03	25	1.1	4–Mar–03
2	29–Mar–03	22–Apr–03	24	1.0	10–Apr–03
3	28–Apr–03	10–May–03	12	0.75	5–May–03
4	26–May–03	3–Jul–03	38	1.1	3–Jun–03

0.1 m^3/s by July (Fig. 9a). Superimposed on this decline, however, were some significant variations, where the trends apparent in the effusion rate data allow the eruption to be split into four periods (Fig. 9a, Table 3).

The first period (Table 3) coincided with the emplacement of the flow field from the 500-m vent. During this period, effusion rates were relatively high (0.6–0.5 m^3/s). However, a slight declining trend was apparent after the middle of January, especially in the week before the shut down of the 500-m vent. Effusion rate declined further during early February from ~0.6 m^3/s on 8–10 February to ~0.3 m^3/s by 13 February (Fig. 2a). This period was thus terminated by a sharp drop in the effusion rate time series coincident with the shut down of the 500-m vent and the subsequent onset of persistent effusion from the 670-m vent (Fig. 9a).

The second period (Table 3) began with a period of moderate (~0.5 m^3/s) effusion rate activity, with a peak around 4 March and lasting until 25 March. At this point, effusion fell, reaching ~0.1 m^3/s by ~24 March. Pulsing behavior characterized the remainder of this period, with two pulses marked by peaks around 10 April and 5 May separated by a trough during 22–28 April (Fig. 9a).

The third period (Table 3) was represented by a short (16 days long) phase of stable but low (~0.1 m^3/s) effusion rate. This was followed by an increase in effusion rate, beginning during 26–27 May, where a final peak of 1.1 m^3/s was reached by 3 June (Fig. 9a). This fourth and final period (Table 3) was terminated by a declining phase, where effusion rates declined to ~0.1 m^3/s by 3 July and remained low until the eruption ended on 21–22 July (Fig. 9a).

Flow lengths

Lengths of individual flow units emplaced during the eruption were generally short, typically <0.5 km, and rarely reaching the coast (Table 3). Like the effusion rate data, our flow length data show a difference between the beginning of the eruption in January, when flows were typically >300 m long, and the remainder of the eruption, when flows were typically <300 m long (Fig. 9b). In addition, the flow length data can be split into the same four periods as applied to the effusion rate time series (Fig. 9b, Table 3).

During the first period, flow lengths were generally high (~400 m, Table 3). However, as with the effusion rate data, a slight declining trend was apparent after the middle of January and preceding the shut down of the 500-m vent. In this study, period 1 was terminated by a marked decrease in flow length data, where flow lengths declined from ~320 m on 7 February to ~160 m by 12–13 February (Fig. 9b). After this period, flows remained relatively short (130–150 m) as activity became focused at the proximal shield fed by the 670-m vents.

This was a period of relatively stable flow lengths and was terminated by a sharp drop on 20 March (Fig. 9b). This marked the end of major exogenous activity during the construction of the proximal tumuli TA–TD, and the beginning of a period when all exogenous activity was focused in the medial–proximal flow sections on the Sciara. Thereafter, and as with the effusion rate data, period 2 was marked by two flow cycles of flow extension, with flow lengths peaking at 240 and 285 m around 16 April and 3 May, respectively (Fig. 9b).

Table 3 Summary of flow field data for each effusive period

Period	Date		Duration (days)	Effusion rate (m^3/s)		Lava flow length		No. of active flows	
	Start	Stop		Mean $\pm 1\sigma$	Maximum	Mean $\pm 1\sigma$ (m)	Maximum (m)	Mean$\pm 1\sigma$	Maximum
1	28/12/02	14/02/03	48	0.6±0.4	1.3	410±80	510	1.8±0.6	3
2	15/02/03	10/05/03	84	0.4±0.3	1.1	185±145	490	2.3±1.2	6
3	11/05/03	27/05/03	16	0.1±0.0	0.1	145±80	250	2.1±1.2	4
4	28/05/03	22/07/03	55	0.3±0.2	1.1	235±135	450	1.9±1.2	4
Total	28/12/02	22/07/03	203	0.32±0.28	1.3	220±150	510	2.1±1.1	6

The third period was marked by generally short (<180 m long) flows, although the trend in flow lengths showed a slight increase, climbing steadily from a low of ~130 m around 11 May to ~170 m by 2 June. Thereafter, the onset of period 4 was marked by an increase in flow length, with lengths increasing rapidly to ~400 m by 11 June (Fig. 9b). Thus, there was a lag between the final increase in effusion rate that marked the onset of period 4 in the effusion rate data on 27 May and the corresponding flow length response. The latter occurred around 2 June, giving a lag of 6–7 days. Thereafter, flow lengths showed the same trend as the effusion rate data, declining to a final low of <100 m by July (Fig. 9b).

Number of active flow units

Although a maximum of six active flow units were observed on 18 March, typically only 1–3 flows were active at any one time (Table 3). However, the relationship between effusion rate and number of active flows was not quite as straightforward as was the case for flow length. During the first activity period when effusion rates and flow lengths were high, number of flows was relatively low and stable (Fig. 9c). This trend continued, until 4 March, straddling the period when activity transferred from the 500-m vent to the 670-m level, a point preceded by a significant decline in effusion rates and flow lengths. After 4 March, the number of active flows showed a steady increase to reach a peak around 18 March. At the same time, effusion rate and flow length both declined suggesting that, at this time, decreased effusion rates were associated with short but complex active flow fields comprising numerous active units.

However, after 20 March, the relationship reversed. Peaks in active flow number occurred during 10–20 April and 5–15 May, with a trough around 5 April. These generally coincided with effusion rate peaks and troughs, respectively (Fig. 9). Thus, over this period, increased effusion rate was associated with increases in flow length and number, so that increased effusion rate resulted in active flow fields that were both longer and more complex, in terms of number of active units, than their low effusion rate counterparts.

During the final period (period 4, Table 3) a lagged relationship was observed between effusion rates, number of active flows, and flow lengths. Effusion rates and active flow number both began to increase during 26–27 May. Peak flow activity, in terms of number of active flows, was observed on 5–6 June, after which time the active flow number declined rapidly to a typical value of 1–2 for the final 40 days of the eruption (Fig. 9). However, flow lengths did not begin to increase until 2 June, peaking around 11 June. Thereafter, all measured parameters showed a declining trend until the end of the eruption (Fig. 9). Thus, at this time, the relationship apparent earlier in the eruption held once more. It seems that this final pulse in effusion was initially spread between many active flow unit, such that no one flow could attain any great distance, building a relatively short but complex compound flow field. However, after 6–7 days, flow became concentrated into just one to three active units, such that these were able to attain greater distances to build a longer but simpler flow field. Thereafter, declining effusion rates caused first flow number and then flow length to decline.

Correlations

The complexities in the qualitative relationships between the three parameters are borne out in the statistical correlations. If we consider the correlations for the entire data set, we obtain a weakly positive linear relationship between flow length (L) and effusion rate (E_r) of $L=357\ E_r+101$, with a poor R^2 of 0.5. We find no correlation between number of active vents (n) and effusion rate.

However, if we consider each of the four effusion rate period defined in Fig. 9 independently, we significantly improve our correlations (Table 4). Generally, effusion rate and flow length show good, if variable, correlations throughout the eruption and improve as the eruption progresses (Table 4). This may reflect a movement away

Table 4 Summary of flow field trends and relationships for each effusive period

Period	Level			Trend			
	E_r (m^3/s)	Length (m)	No. of flows	E_r	Length	Correlation	R^2
1 (28/12–14/02)	High (0.6)	High (414)	Low (1.8)	Decreasing	Decreasing	$L=726 \times E_r-104$	0.48
2a (15/02–20/03)	Moderate (0.5)	Low (137)	Low (1.8)	First pulse	First pulse	$L=-265 \times E_r+265$	0.77
2b (21/03–10/05)	Moderate (0.3)	Low (179)	Moderate (2.3)	Pulsing	Pulsing	$L=545 \times E_r+30$	0.65
3 (11/05–27/05)	Low (0.1)	Low (143)	High (2.6)	Steady	Slight increase	None	–
4a (28/05–07/06)	Moderate (0.4)	Low (158)	High (2.8)	Increasing	Increasing	$L=519 \times E_r+3$	0.89
4b (08/06–11/06)	Moderate (0.4)	High (417)	Moderate (2.0)	Decreasing	Increasing	$L=-364 \times E_r+511$	0.99
4c (12/06–20/07)	Low (0.2)	Low (242)	Low (1.6)	Decreasing	Decreasing	$L=1121\times E_r+35$	0.98

from vent-dominated activity to flow-field-dominated activity. This would favor a focusing of exogenous effusive activity, and hence the volume flux, on the Sciara and in the medial and distal flow field zones. Thus, as flow became concentrated in one location, more direct relationships between effusion rate and flow length began to operate.

During period 1, when activity was focused at the 500-m vent, the correlation between effusion rate and flow length poor (R^2~0.5). This may be explained by constant crumbling of flow fronts on the steep slopes. In the past, such empirical relationships have been shown to rely on flow fronts reaching their maximum cooling-limited extent (Calvari and Pinkerton 1998; Wright et al. 2001). Flow front failure will cause mechanical flow shortening and result in flows that are rarely able to attain their maximum cooling-limited length, where variable amounts of failure will result in variable relationships depending on whether flow lengths are acquired just before or after a major collapse.

During the first half of the second period, flow lengths were generally low inspite of moderate effusion rate, and effusion rate was negatively correlated with flow length and number. During this period, the main tumuli (TA, TB, TC, and TD) were being constructed at the proximal shield. Thus, a portion of the effused lava would have contributed to shield construction as well as flow field construction, complicating any straightforward relationship between effusion rate and flow length by robbing flows of supply and causing them to be, on occasion, volume-limited.

During the final period (3), there was generally improved (R^2>0.6) positive correlation between effusion rate and flow length. The only exception was a short period during 8–11 June when flow lengths and effusion rates were negatively correlated (Table 4: period 4b). As already discussed, this resulted from a lagged flow length response to the final effusion pulse due to the initial flux being widely distributed across numerous active flow units.

Discussion

The underlying slope on which the 2002–2003 flow field at Stromboli was emplaced resulted in a characteristic flow field morphology. Broadly, this was comprised of a proximal shield, across which flow stacking and inflation caused a piling up of lava on the relatively flat ground of the vent zone. Tube channel-fed flow from this proximal zone fed a second flow field zone in the medial–distal zone. The medial–distal flow field was emplaced on extremely steep slopes, and this had two effects. First, it caused flows to slide as well as flow and, second, it promoted lava flow front crumbling to result in the production of an extensive debris field.

Flow front crumbling due to toe failure at lavas advancing on steep slopes was described for Etna lavas more than a century ago (Lyell 1858), and is in general considered responsible for autobrecciated lava flows (Borgia et al. 1983; Calvari et al. 1994) that produce a distal talus of breccia. Such deposits show clast sorting by gravity, characterized by a thinner and fine-grained deposit close to the source, and a coarser, thicker debris further down slope (Tanner and Hubert 1991). Accumulation of fine-grained debris in the proximal zone, in turn, increases the possibility of excavated levee formation (Calvari et al. 2006), favoring the establishment of well-confined lava channels. If effusion rate is stable for long enough to allow roof sealing, lava tubes develop along this path. Alternatively, tubes form even faster when lava flows become covered by debris. The resulting deposit of this activity would be a complex pile of debris alternating with lava flows.

Flow front crumbling has an additional effect. By converting lava flows to debris flow, much of which, in this case, was lost to the sea; the final flow field is robbed of significant volume. Thus, the final volume of such a flow field may not represent the actual volume of erupted lava. It is interesting to note that as of June 2004, the morphology of the Sciara in the vicinity of the 2002–2003 flow field was an ashy slope, with no sign of the lava flows that have been observed as active in the same location a year earlier, much of the initial lava flow material having crumbled and fallen into the sea by avalanche or grain flow. Thus, the flow field volume is now much less than the total-erupted volume. The June 2004 volume of 2002–2003 flow field on the Sciara del Fuoco was ~2×10^6 m^3. This compares with ~6×10^6 m^3 obtained by integrating the smoothed effusion rate data (Calvari et al. 2005). Thus, around 4×10^6 m^3 of this flow field (~70% of the total erupted volume) may have been removed by collapse.

Flow front collapse also causes problems when correlating flow length with effusion rate. Through mechanical truncation, flow collapse violates the assumption that all flow units attain their cooling limited extent. In addition, collapse and failure of channel levees may cause flow diversion before a unit can attain its cooling limited maxima, again violating the assumption and introducing noise such that R^2 values are low and variable.

Three other factors complicate a direct relationship between effusion rate and flow length, the first two of which complicate the assumption that total effusion rate is concentrated in one flow unit. First, where more than one vent is active, the volume flux will be distributed between multiple vents to feed several short flows within the vent area as well as flows into the medial–distal flow zone. Second, where more than one flow is active within the medial–distal zone, again the volume flux will be distributed between flows. In both cases, shorter flows will result

than had the volume flux be concentrated in a single flow. It may thus be more reasonable to consider the local effusion rate feeding the flow whose length is being considered, rather than using the total flux estimate. Finally, although extensive, our data set is incomplete. Thus, for example, if we have a long lava flow on a certain day that correlates with a low effusion rate, it may be responding to a higher effusion rate that was unmeasured in the previous (unobserved) days to hours.

Effusion rate trends and 5 April

The effusion rate data show a general decline in erupted flux between 7 January and 4 April. This is best revealed in the weekly average and maxima data. These show a 12-week-long linear decline during January–April (Fig. 2b, c). This first period of decline was terminated by the 5 April paroxysm. After this date, effusion rates recover to be followed by a second 7-week-long linear decline (Fig. 2b, c). This second decline is terminated by another sudden increase in effusion rate around 31 May–3 June. This correlates with a short period of intense strombolian and fountaining activity from the summit craters. Effusion rates then follow a third and final period of linear decline, again lasting 7 weeks and terminating with the end of the eruption (Fig. 2b, c). It thus appears that three periods of steady effusion rate decline are each terminated with a significant event: the 5 April explosive, the early-June explosive activity, and the eruption end, respectively.

Superimposed on these trends, we observe short-lived effusion rate pulses. The first occurred during 4–11 March (Fig. 9a), a period during which a significant increase in strombolian activity was observed, where the number of strombolian events recorded on day time (6 a.m.–6 p.m., local time) digital images from the INGV-CT monitoring web camera increased from two on 4 March to 28, 82 and 130 on 5, 6, and 7 March, before returning to a typical level of two on 8 March. The second and third pulses occurred around 5 April and 5 May (Fig. 9), respectively, when two further increases in explosive activity were observed, the first being associated with the major explosive paroxysm of 5 April.

It thus appears that the apparently persistent effusion was fed by the arrival of three major batches around 28 December, 5 April and May 31. Each was associated in a major increase in explosive activity and/or a revival of the effusion rates, and was followed by a period of steady decline. Superimposed on these are two shorter periods when effusion rate and explosive activity increased for just a few days. We suggest that these might be associated with the arrival of smaller batches. All of these was superimposed on a general, long-term, declining trend that persisted throughout the eruption (Fig. 9a).

Conclusion

The Stromboli 2002–2003 effusive eruption was a relatively persistent (7 months long), but low effusion rate (<1 m^3/s) eruption, with a time averaged dense rock effusion rate of 0.32 m^3/s. The flow field, however, showed systematic variations in effusion rate, vent number, and location. Generally, the behavior was pulsed, with four ~20-day long pulses in lava flow activity apparent after February 15. In addition, the morphology of vent structures and flows showed a number of characteristic features that were a result of the slopes in which they were emplaced. Most notable was the emplacement of channel and tube fed, sliding and flowing ′a′a units that suffered near constant failure to feed debris flows. In this study, if we were to cut the surviving (noncollapsed) portion of the debris flow in the across-flow field direction, we would obtain a section that comprised a series of thin ′a′a flow units separated by layers of debris deposits. If we were to make the same section in the downflow direction, we would observe the same sequence, but debris deposits would become thicker and lava flow units rarer in the downflow direction.

Thus, our observations provide a framework within which past and future lava flow eruptions over steep slopes can be measured, interpreted, and understood. The use of the FLIR to gain daily images of the flow field proved valuable in constraining the evolution and morphology of this flow field. Thus, such hand-held thermal remote sensing tools should also be used in cases where close approach is possible, as well as in cases where approach is difficult. In this study, the image data allow spatially (and temporally) detailed synoptic, flow wide coverage and consideration.

Acknowledgements We are indebted to all colleagues of INGV from Catania, Palermo, Napoli, Roma, and Milano that helped during monitoring as well as to Maurizio Ripepe (University of Florence) for extensive discussions, as well as the Air Walser and Civil Protection helicopter pilots that made our data collection possible. Massimo Cascone is thanked for his help with figure preparation. We also gratefully acknowledge the support of the Italian Civil Protection Department to our activities. SC, LL, and LS wish to thank Alessandro Bonaccorso, Giovanni Macedonio, and Enzo Boschi for continuous support and encouragement throughout the eruption. AJLH, JD, and MP were funded by INGV-Catania, NSF grant EAR-0207734 and the Alaska Volcano Observatory.

References

Bonaccorso A, Calvari S, Garfì G, Lodato L, Patané D (2003) Dynamics of the December 2002 flank failure and tsunami at Stromboli volcano inferred by volcanological and geophysical observations. Geophys Res Lett 30:1941. DOI 10.1029/2003GL017702

Borgia A, Linneman S, Spencer D, Morales LD, Andre JB (1983) Dynamics of lava flow fronts, Arenal volcano, Costa Rica. J Volcanol Geotherm Res 19:303–329

Calvari S, Pinkerton H (1998) Formation of lava tubes and extensive flow field during the 1991–93 eruption of Mount Etna. J Geophys Res 103:27291–27302

Calvari S, Pinkerton H (1999) Lava tube morphology on Etna and evidence for lava flow emplacement mechanisms. J Volcanol Geotherm Res 90:263–280

Calvari S, Coltelli M, Neri M, Pompilio M, Scribano V (1994) The 1991–93 Etna eruption: chronology and geological observations. Acta Vulcanol 4:1–15

Calvari S, Spampinato L, Lodato L, Harris AJL, Patrick MR, Dehn J, Burton MR, Andronico D (2005) Complex volcanic processes observed with a hand-held thermal camera during the 2002–2003 flank eruption at Stromboli volcano (Italy). J Geophys Res 110: B02201. DOI 10.1029/2004JB003129

Calvari S, Spampinato L, Lodato L (2006) The 5th April 2003 vulcanian explosion at Stromboli reconstructed from visual observation and thermal data. J Volcanol Geotherm Res 149:160–175

Cigolini C, Borgia A, Casertano L (1984) Intra-crater activity, aa-block lava, viscosity and flow dynamics: Arenal volcano, Costa Rica. J Volcanol Geotherm Res 20:155–176

De Fino M, La Volpe L, Falsaperla S, Frazzetta G, Neri G, Francalanci L, Rosi M, Sbrana A (1988) The Stromboli eruption of December 6, 1985–April 25, 1986: volcanological, petrological and seismological data. Rend Soc Ital Mineral Petrol 43:1021–1038

Duncan A M, Guest JE, Stofan ER, Anderson SW, Pinkerton H, Calvari S (2004) Development of tumuli in the medial portion of the 1983 aa flow-field, Mount Etna, Sicily. J Volcanol Geotherm Res 132:173–187. DOI 10.1016/S0377-0273(03)00344-5

Harris AJL, Murray JB, Aries SE, Davies MA, Flynn LP, Wooster MJ, Wright R, Rothery DA (2000) Effusion rate trends at Etna and Krafla and their implications for eruptive mechanisms. J Volcanol Geotherm Res 102:237–270

Harris AJL, Dehn J, Patrick MR, Calvari S, Ripepe M, Lodato L (2005) Lava effusion rates from hand-held thermal infrared imagery: an example from the June 2003 effusive activity at Stromboli. Bull Volcanol 68:107–117

Hon K, Kauahikaua J, Denlinger R, Mackay K (1994) Emplacement and inflation of pahoehoe sheet flows: observations and measurements of active lava flows on Kilauea Volcano, Hawaii. Geol Soc Amer Bull 106:351–370

Kilburn CRJ, Guest JE (1994) Aa lavas of Mount Etna, Sicily. In: Kilburn CRJ, Luongo G (eds) Active lavas: monitoring and modelling. UCL Press, London, pp 73–106

Kilburn CRJ, Lopes RMC (1988) The growth of aa lava flow fields on Mount Etna, Sicily. J Geophys Res 93:14759–14772

Kilburn CRJ, Lopes RMC (1991) General patterns of flow field growth: aa and blocky lavas. J Geophys Res 19:721–19732

Kokelaar BP, Romagnoli C (1995) Sector collapse, sedimentation and clast population evolution at an active island-arc volcano: Stromboli, Italy. Bull Volcanol 57:240–262

Lipman PW, Banks NG (1987) Aa flow dynamics, Mauna Loa 1984. US Geol Surv Prof Pap 1350:1527–1567

Lyell C (1858) On the structure of lavas which have consolidated on steep slopes; with remarks on the mode of origin of Mount Etna, and on the theory of "craters of elevation". Philos Trans R Soc Lond 148:703–786

Mattox TN, Heliker C, Kauahikaua J, Hon K (1993) Development of the 1990 Kalapana Flow Field, Kilauea Volcano, Hawaii. Bull Volcanol 55:407–413

Peterson DW, Holcomb RT, Tilling RI, Christiansen RL (1994) Development of lava tubes in the light of observations at Mauna Ulu, Kilauea Volcano, Hawaii. Bull Volcanol 56:343–360

Pino NA, Ripepe M, Cimini GB (2004) The Stromboli volcano landslides of December 2002: A seismological description. Geophys Res Lett 31:L02605. DOI 10.1029/2003GL018385

Polacci M, Papale P (1997) The evolution of lava flows from ephemeral vents at Mount Etna: insights from vesicle distribution and morphological studies. J Volcanol Geotherm Res 76:1–17

Ripepe M, Marchetti E, Poggi P, Harris AJL, Fiaschi A, Ulivieri G (2004) Seismic, acoustic, and thermal network monitors the 2003 eruption of Stromboli Volcano. EOS Trans AGU 35:329–332

Ripepe M, Marchetti E, Ulivieri G, Harris AJL, Dehn J, Burton MR, Caltabiano T, Salerno G (2005) Effusive to explosive transition during the 2003 eruption of Stromboli volcano. Geology 33:341–344. DOI 10.1130/G21173.1

Rossi MJ, Gudmundsson A (1996) The morphology and formation of flow-lobe tumuli on Icelandic shield volcanoes. J Volcanol Geotherm Res 72:291–308

Swanson DA (1973) Pahoehoe flows from the 1969–1971 Mauna Ulu eruption, Kilauea volcano, Hawaii. Geol Soc Amer Bull 84:615–626

Tanner LH, Hubert JF (1991) Basalt breccias and conglomerates in the lower Jurassic McCoy Brook Formation, Fundy Basin, Nova Scotia: differentiation of talus and debris-flow deposits. J Sed Petrol 61:15–27

Walker GPL (1991) Structure and origin by injection of lava under surface crust of tumuli, "lava rises", "lava-rise pits", and "lava-inflation clefts" in Hawaii. Bull Volcanol 53:546–558

Wright R, Flynn LP, Harris AJL (2001) Evolution of lava flow-fields at Mount Etna, 27–28 October 1999, observed by Landsat 7 ETM+. Bull Volcanol 63:1–7